Received: 21 February 2021 | Revised: 19 March 2021 | Published online: 19 April 2021

DOI: 10.1002/trc2.12170

Alzheimer's & Dementia
Translational Research & Clinical Interventions

RESEARCH ARTICLE

Inhibition of Tau aggregation with BSc3094 reduces Tau and decreases cognitive deficits in rTg4510 mice

Marta Anglada-Huguet[1,2,§] | **Sara Rodrigues**[1,2,§] | **Katja Hochgräfe**[1,2] | **Eckhard Mandelkow**[1,2] | **Eva-Maria Mandelkow**[1,2]

[1] German Center for Neurodegenerative Diseases, DZNE, Bonn, Germany

[2] Center for Advanced European Studies and Research, CAESAR, Bonn, Germany

Correspondence
Eva-Maria Mandelkow, DZNE, German Center for Neurodegenerative Diseases, Venusberg-Campus 1, Building 99, 53127 Bonn, North Rhein Westphalia, Germany.
Email: Eva.Mandelkow@dzne.de

Marta Anglada-Huguet, DZNE, German Center for Neurodegenerative Diseases, Venusberg-Campus 1, Building 99, 53127 Bonn, North Rhein Westphalia, Germany.
Email: Marta.Anglada@dzne.de

Funding information
This project has received funding from German Center for Neurodegenerative Diseases(DZNE), Max-Planck-Society (MPG), EU Horizon 2020 research program (No676144, SyDAD), Katharina-Hardt-Foundation, and Cure Alzheimer's Fund.

[§]Marta Anglada-Huguet and Sara Rodrigues contributed equally to this work

Abstract

Background: One of the major hallmarks of Alzheimer's disease (AD)is the aberrant modification and aggregation of the microtubule-associated protein Tau . The extent of Tau pathology correlates with cognitive decline, strongly implicating Tau in the pathogenesis of the disease. Because the inhibition of Tau aggregation may be a promising therapeutic target, we tested the efficacy of BSc3094, an inhibitor of Tau aggregation, in reducing Tau pathology and ameliorating the disease symptoms in transgenic mice.

Methods: Mice expressing human Tau with the P301L mutation (line rTg4510) were infused with BSc3094 into the lateral ventricle using Alzet osmotic pumps connected to a cannula that was placed on the skull of the mice, thus bypassing the blood-brain barrier (BBB) . The drug treatment lasted for 2 months, and the effect of BSc3094 on cognition and on reversing hallmarks of Tau pathology was assessed.

Results: BSc3094 significantly reduced the levels of Tau phosphorylation and sarkosyl-insoluble Tau. In addition, the drug improved cognition in different behavioral tasks and reduced anxiety-like behavior in the transgenic mice used in the study.

Conclusions: Our in vivo investigations demonstrated that BSc3094 is capable of partially reducing the pathological hallmarks typically observed in Tau transgenic mice, highlighting BSc3094 as a promising compound for a future therapeutic approach for AD.

KEYWORDS
aggregation inhibitor, Alzet pump, Alzheimer's disease, BSc3094, P301L Tau mutation, Tau pathology

1 | INTRODUCTION

Alzheimer's disease (AD) is a progressive age-related neurodegenerative disorder, characterized by impairments in memory and behavior. The high prevalence of the disease, related to the increased life expectancy, is prompting governments and scientists around the world to increase research and clinical efforts to search for novel therapeutic targets for AD.

The two major histopathological hallmarks of the disease are the extracellular deposition of senile plaques composed of amyloid beta (Aβ) and the aberrant phosphorylation and aggregation of the microtubule (MT)–associated protein (MAP) Tau (*MAPT*) in neuronal cells,

This is an open access article under the terms of the Creative Commons Attribution-NonCommercial-NoDerivs License, which permits use and distribution in any medium, provided the original work is properly cited, the use is non-commercial and no modifications or adaptations are made.
© 2021 The Authors. *Alzheimer's & Dementia: Translational Research & Clinical Interventions* published by Wiley Periodicals, Inc. on behalf of Alzheimer's Association.

leading to the formation of neurofibrillary tangles (NFTs).[1,2] Due to the failure of several Aβ-directed therapies, the development of novel therapeutic interventions is shifting toward drugs targeting Tau protein[3]

Tau belongs to the family of MAPs[4] Tau protein is expressed mainly in the axons of mature and growing neurons,[5] although it is also present at lower levels in astrocytes and oligodendrocytes.[6,7] The protein plays a central role in MT stabilization and in the regulation of MT dynamics and axonal transport.[8,9]

During the clinical course of AD, filamentous Tau inclusions appear sequentially throughout the brain following a stereotypical pattern, providing the basis for disease staging as described by Braak.[10] Braak stages I and II correspond to the appearance of NFTs in the transentorhinal and entorhinal cortex (EC) and are not associated with clinical dementia. More-pronounced involvement of the entorhinal region and formation of NFTs in the hippocampus are characteristics of stages III and IV, where the first clinical symptoms appear (mild cognitive impairment). At the later stages of the disease (Braak stages V and VI) Tau pathology has extensively reached the neocortex, and patients are severely demented, meeting the neuropathological criteria for the diagnosis of AD.[10,11]

Although the mechanisms underlying Tau-mediated neurotoxicity in AD are still not well understood, multiple therapeutic approaches have been proposed that target Tau function or dysfunction, based on the current understanding of these mechanisms.[12–14]

Therapies, directly or indirectly targeting Tau protein, are being tested in preclinical and clinical studies and include:

1. Tau aggregation blockers to inhibit aberrant aggregation; for example, methylene blue (MB) or derivatives, which were shown to induce autophagy and attenuate tauopathy in vitro and in vivo[11,15–19]; PE859 (curcumin based compound), AZP2006 (piperazine-derived drug)[14] or LMTX (Leucomethylene blue reduced form of MB).[20,21]
2. Reduction of Tau levels to inhibit aggregation or interactions with cell components (eg, siRNA or antisense oligonucleotides targeting Tau).[22–24]
3. Vaccination to neutralize toxic Tau species (eg, passive: antibodies PHF-1 or MC1; active: advacc1, a vaccine developed against the repeat domain of Tau).[25–28]
4. Targeting enzymes that regulate Tau post-translational modifications (PTMs) (eg,
5. Kinase inhibitors or phosphatase enhancers to reduce the level of phosphorylation[29]
6. HDAC6 (histone deacetylase 6) inhibitor.[30–33]
7. Targeting autophagy or proteasomes to promote Tau degradation (eg, autophagy inducers).[34,35]
8. MT stabilizers to compensate the loss of stabilization by Tau (eg, Paclitaxel, curcumin).[36,37]

BSc3094 monohydrobromide (2-[4-(4-nitrophenyl)-2-thiazolyl]hydrazide-1H-benzimidazole-6-carboxylic acid monohydrobromide) is a phenylthiazolyl-hydrazide derivative developed by B. Schmidt and colleagues as a potent Tau aggregation inhibitor.[38] Previous studies have demonstrated a high efficacy in reducing both Tau aggregation and phosphorylation, while increasing cell viability and having no cytotoxic effects in an in vitro N2a cell model expressing pro-aggregant mutant hTau,[39,40] as well as in a *C. elegans* model of tauopathy expressing pro-aggregant mutant hTau.[17] Recently, BSc3094 reversed the pre-synaptic impairment in organotypic hippocampal slices from pro-aggregant mice, by reversing the paired-pulse depression observed in non-treated pro-aggregant Tau slices after applying a paired-pulse stimulus of the Schaffer collaterals.[41] Taken together, these results strengthen the hypothesis that BSc3094 could be a therapeutic agent to reverse Tau pathology and, possibly, exert a beneficial effect in AD.

Aiming to extend the potential therapeutic effect of BSc3094 to an *in vivo* mouse model, we administered the drug in rTg4510 mice, expressing human Tau (hTau) with the P301L mutation. Because the blood-brain barrier (BBB) represents a major obstacle to the delivery of BSc3094 into the central nervous system (CNS), we used Alzet osmotic pumps to directly deliver the drug in the lateral ventricle of the mouse brain. Cognitive performance and markers of Tau pathology were assessed at the end of the drug treatment.

RESEARCH IN CONTEXT

1. **Systematic review:** Low-molecular-weight compounds aiming at Tau aggregation may be potential drugs for Alzheimer's disease (AD) pathology. Earlier screens identified promising compounds, including (BSc3094), which potently inhibited Tau aggregation in vitro, *Caenorhabditis elegans* models, or organotypic slices from mouse models. However, it crossed the blood-brain barrier only poorly.
2. **Interpretation:** We used Alzet pumps for a 4-week application of BSc3094 directly to brains of rTg4510 mice at the onset of cognitive decline. Treatment was remarkably efficient in reducing biochemical hallmarks (Tau aggregation, phosphorylation) and some behavioral parameters.
3. **Future direction:** Results show that BSc3094 can partly reverse tauopathy. This justifies future research on brain-penetrant derivatives of the compound.

2 | MATERIALS AND METHODS

2.1 | Animals

All animal experiments were carried out in accordance with the guidelines of the German Welfare Act and approved by the local authorities (Landesamt für Natur, Umwelt und Verbraucherschutz Nordrhein-Westfalen) under animal permission 84-02.04.2017-A405. Animals were housed in groups of 2-5 animals under standard conditions (23°C,

40% to 50% humidity, *ad libitum* access to food and water) with a 12-hour light/dark cycle (with light on from 6 a.m. to 6 p.m.).

The transgenic mouse model rTg4510 was used, expressing the Tau isoform 0N4R (Uniprot P-10636-D, alias "hTau24", 383 residues) with the fronto temporal dementia linked with parkinsonism 17 (FTDP17) mutation P301L[42,43]. Briefly, rTg4510 animals were produced by crossing the activator mouse line CamKII-tTA, with the responder tetO.MAPT*P301L mouse line. Mice having both CamKII-tTA and Tau transgene expressed human mutant P301L Tau at high levels, up to ≈13 time endogenous Tau. Mice lacking the responder and the activator transgene were used as controls. Mice were screened by PCR using the following primer pairs: hTau transgene (Tau mPrP_E2): forward 5′-TGA ACC ATT TCA ACC GAG CTG-3′; reverse: 5′-TAC GTC CCA GCG TGA TCT TC-3′; CamKII promoter (oIMR8746/oIMR8747): forward 5′-CGC TGT GGG GCA TTT TAC TTT AG-3′; reverse: 5′-CAT GTC CAG ATC GAA ATC GTC-3′.

2.2 | BSc3094 concentration in the brain

To determine the ability of BSc3094[38] to cross the BBB, intravenous (i.v.) injections of BSc3094 (Sigma-Aldrich, 3 mg/kg in PEG400/water (60:40)) were performed in wild-type (WT) animals, and the concentration of the drug in the brain was estimated up to 24 hours post-dose.

2.3 | Implantation of Alzet osmotic pumps

Alzet osmotic pumps (Alzet, model 1004; volume: 100μL; infusion rate: 0.11μL/h; duration: 28 days) combined with the Alzet brain infusion kit three were implanted into anesthetized rTg4510 and control non-transgenic mice, as described previously.[22]

To determine the BSc3094 dose to be used in the therapeutic approach, Alzet osmotic pumps containing vehicle (PEG400:ddH_2O (60:40)) or three different concentrations of BSc3094 (0.075, 0.150 and 1.5 mM) were implanted in 2-month-old rTg4510 mice for direct infusion of the drug into the brain, on the onset of cognitive decline. The treatment lasted 28 days, after which the brain tissue was collected and total Tau levels were analyzed by western blot in the sarkosyl-insoluble fraction, obtained from cortical extracts, to determine the most effective dose in reducing the levels of sarkosyl-insoluble Tau.

After determining the experimental dose, the therapeutic approach started. Alzet osmotic pumps were filled with 100 μL of BSc3094 (1.5 mM in 60:40 PEG400/ddH_2O) or vehicle (60:40 PEG400/ddH_2O).

2.4 | Behavioral assessment

2.4.1 | Nesting test

Mice were single-housed with one nestlet per cage,[44,45] and the percentage of nesting was monitored at different time points (2 and 6 hours and overnight [ON]). After each assessment, a new nestlet was placed in the cage, instead of keeping the same nestlet for the following time point. The percentage of nesting was assessed at each time point (% nesting = 100-(([final weight]/[initial weight]) × 100)), and nest-building scores were defined by the following criteria:

0, nestlet untouched

1, less than 10% of the nestlet was shredded

2, 10% to 50% of the nestlet was shredded but there was no shape in the nest

3, 10% to 50% of the nestlet was shredded and there was shape in the nest

4, 50% to 90% of the nestlet was shredded but there was no shape in the nest

5, 50% to 90% of the nestlet was shredded and there was shape in the nest

6, >90% of the nest was shredded, but the nest was flat

7, >90% of the nest was shredded, and the walls of the nest were at least as tall as the mouse on more than 50% of its sides.

2.4.2 | Burrowing test

Mice were single-housed and a plastic downpipe (68 mm diameter; 20 cm long) with one open and one closed end was placed in the cage, as described previously.[45,46] The tube was filled with 200 g of the food pellets normally supplied as diet. Machine screws were used to elevate the open end of the tube 3 cm off the floor to prevent accidental displacement of the food pellets. The test started at ≈4 pm, 2 hours before the dark period in the holding room. The final food pellets weight was measured the next morning and the percentage of burrowing determined (% burrowing = 100-((final weight)/(initial weight)) × 100).

2.4.3 | Open field (OF) test

Mice were placed in the center of a 50 × 50 cm arena divided into 20 × 20 cm center, a 5 cm wall zone, and a 10 cm border zone, and allowed to explore the arena freely for 10 minutes while being tracked by a video system (EthoVision XT, Noldus Information Technology). The distance traveled and the time spent in the center zone were analyzed.

2.4.4 | Novel object recognition (NOR) test

Mice were tested in a square open field arena (50 × 50 cm) (Panlab, Spain) located in a room with dim lighting, as described previously.[41] Briefly, after habituation to the OF arena (10 min/day over 2 days; no objects), the mice were placed in the open field with two identical objects for 10 minutes. To assess long-term memory, 24 hours later the mice were placed again in the OF arena for 5 minutes and one of the familiar objects was replaced by a novel one. To record and analyze behavior, the EthoVision XT video tracking system was used (Noldus Information Technology).

2.4.5 | Y-maze test

The Y-maze behavioral test was used to assess hippocampus-dependent memory. The Y-maze used had the dimensions length 30 cm; width 6 cm; height 15 cm (Panlab, Spain). The test was divided in two parts, as described[41]: the training session and the test session. During the training, one of the arms of the maze was closed (novel arm), and the mice were placed in the stem arm of the Y-maze (home arm), and allowed to explore this and the other available arm (old arm) for 10 minutes. After exploration, the mice were placed back in their home cage. Four hours later, the closed arm was opened, and the mice were placed in the stem arm of the Y-maze and allowed to freely explore all the arms for 5 minutes, to assess long-term memory. To record and analyze behavior the EthoVision XT video tracking system was used (Noldus Information Technology).

2.4.6 | Morris Water Maze (MWM) test

The MWM test was conducted to assess spatial working memory, as described previously.[47,48] Briefly, the test was performed as follows:

2.4.7 | MWM pre-training

Two days pre-training protocol to familiarize the mice with swimming and climbing to a hidden platform (22°C water temperature, four trials/day, maximum trial duration 60 seconds, 20 minutes inter-trial interval). The pre-training was performed in a laboratory sink, and not in the apparatus used for the MWM (circular pool, diameter of 150 cm), to avoid interference with the MWM learning. The pre-training platform (10 cm diameter) was placed 1 cm below the water surface.

2.4.8 | MWM acquisition and probe trials

A 150 cm circular pool was filled with water opacified with non-toxic white paint (Biofa Primasol 3011, Germany) and kept at 22°C, as described previously.[49] In the middle of the target quadrant, a 15 cm round platform was hidden (1 cm beneath the water surface). The MWM room was equipped with visual cues to facilitate orientation. The pool was divided into four quadrants: target (T), right adjacent (R), opposite (O), and left adjacent (L). Each mouse performed four swimming trials per day (maximum duration 60 seconds, 15 to 20 minute inter-trial interval) for 5 consecutive days. Mice started the test from four symmetrical positions in a pseudo-randomized order across trials. When mice failed to find the submerged platform within 60 seconds, they were guided to the platform, remaining there for 15 seconds before returning to their cage. The escape latency, the distance traveled, and swimming speed were determined. On acquisition days 3, 4, and 5, and for 3 days after the end of the acquisition phase (day 8), a probe trial was conducted by removing the platform and recording the search pattern of the mice for 60 seconds. The following learning trials 3 to 4 were carried out with the platform placed in the initial position on the target quadrant to avoid extinction. During acquisition and probe trials the EthoVision XT video tracking system was used (Noldus Information Technology).

2.5 | Brain homogenization and protein quantification

After sacrificing the mice by cervical dislocation, the brains were collected immediately and dissected for western blot and sarkosyl extraction. Lysis buffer (50 mM Tris-HCl, 10% Glycerol, 1% NP40, 5 mM DTT, 1 mM NaEGTA/EGTA, 20 mM NaF, 1 mM Na_3VO_4, 150 mM NaCl, 1x complete mini 25x protease inhibitor [Sigma-Aldrich], 5 mM CHAPS, 100 U Benzonase, 5 μM okadaic acid, 2 mM ddH_2O, 1 mM PMSF) was added to each Eppendorf tube containing the dissected brain tissues and samples were sonicated 5 seconds (amplitude 40%) followed by another sonication of 3 seconds. Samples were kept in ice for 20 minutes, centrifuged 20 seconds at 14,000 rpm (Eppendorf centrifuge 5415R), and the supernatant was collected. Protein concentration was estimated using 1 μL of the supernatant and a Bicinchoninic Acid Protein assay kit (Sigma-Aldrich, Germany).

2.6 | Sarkosyl extraction

A sarkosyl-insoluble Tau fraction was isolated from brain tissue as described previously.[50,51] Briefly, the brain tissue was weighed, homogenized in three times volume of cold Buffer H (10 mM Tris-HCl, 1 mM EGTA, 0.8 M NaCL, 10% sucrose, pH 7.4), and centrifuged at 26,000 rpm (Beckman CoulterTM Optima TM MAX-E) for 20 minutes at 4°C. The supernatant was collected, and the resulting pellet was homogenized in buffer H and centrifuged at 26, 000 rpm for 20 minutes at 4°C. Both supernatants were combined, adjusted to 1% (w/v) N-lauroylsarcosine and incubated at 37°C with shaking for 2 hours. After centrifugation at 61,000 rpm for 35 minutes at 20°C, the supernatant was collected (sarkosyl-soluble fraction) and the pellet was resuspended in 500 μL of 1x TBS and centrifuged again at 61,000 rpm for 35 minutes at 20°C, the supernatant removed, and the pellet resuspended in 0.5 μL onetime TBS for each mg of original sample plus the same amount of two times sample buffer and samples stored for SDS gel. Western blotting was used to analyze the supernatant (sarkosyl-soluble fraction) and the pellet (sarkosyl-insoluble fraction).

2.7 | Western blotting

Homogenized brain tissue (hippocampus), plus sarkosyl-soluble and -insoluble fractions (cortex) were resolved in 10% SDS-PAGE gels, followed by semi-dry transfer to PVDF membranes. Primary antibody incubation was performed overnight at 4°C in TBS-T (Tris-buffered saline, 0.1% Tween 20). The following primary antibodies were used:

12E8 (1:2000, ELAN Pharmaceuticals), PHF-1 (1:1000, kind gift from Dr. P. Davies), K9JA (1:20 000, DAKO), PSD95 (1:1000, Cell signaling), Synaptophysin (1:5000, Sigma-Aldrich), and GluR1 (1:1000, Merck). After being washing 3x in TBS-T plus 5% non-fat dry milk, the membranes were incubated with secondary antibodies for 1 hour at RT (anti-mouse 1:2000, or anti-rabbit 1:2000, DAKO). Antibody affinity was detected by chemiluminescence with Amersham ECL Prime Western Blotting Detection Reagent (GE Healthcare, Germany). Protein bands were visualized using Image Quant LAS 4000 mini (GE Healthcare Life Sciences, Germany), and band intensities were analyzed using Image Studio Lite 5.2 software (LI-COR Biosciences). Actin (1:10 000, Sigma-Aldrich) and β-III-tubulin (1:5000, RD Systems) were used as loading controls.

2.8 | Statistical analysis

For western blotting, the mean density and area of each band were measured using at least three independent experiments and quantified by a computer-assisted densitometer (Gel-Pro Analyzer, version 4; Media Cybernetics, Bethesda, MD, USA). The statistical analysis was completed using Graph Pad (Prism) version 7.05 software. All values are given as mean ± standard error of the mean (SEM). To compare the experimental groups a one-way or two-way analysis of variance (ANOVA) was performed, with uncorrected Fisher's least significant difference (LSD) or Tukey's post hoc test for multiple comparisons to evaluate statistical significance. Differences were considered statistically significant when $P < .05$.

For behavioral assessment, statistical comparisons between groups were accomplished by one-way or two-way ANOVA followed by post hoc uncorrected Fisher's LSD or Tukey's multiple comparison tests. All data are presented as group mean values ± SEM. The accepted level of significance was $P < .05$. Statistical comparisons and graphs were performed using Graph Pad (Prism) version 7.05 software. $^{*}P < .05$, $^{**}P < .01$, $^{***}P < .001$, $^{****}P < .0001$.

3 | RESULTS

3.1 | BSc3094 has poor BBB permeability, but direct intraventricular administration reduces sarkosyl-insoluble Tau

Administration of BSc3094 through intravenous injection (3 mg/kg, in PEG400/ddH_2O (60:40)) showed that the compound has poor BBB permeability, as the concentration reaching the brain was very low (≈70 ng/mL). Furthermore, the half-life of the drug in the brain corresponded to 0.8 hours (Figure 1A), meaning that it is not suitable for a brain-related disease therapeutic approach. Nevertheless, taking into account the optimistic results obtained previously,[17,39,41] we hypothesized that local delivery of BSc3094 into the brain could produce therapeutic effects. Therefore, we used Alzet osmotic pumps to directly deliver three different doses of BSc3094 (0.075, 0.150, and 1.5 mM) in the lateral ventricle of rTg4510 mice continuously over 28 days. As shown in Figure 1B, administration of 1.5 mM of BSc3094 reduced the levels of sarkosyl-insoluble Tau in cortical extracts by ≈70%. This dose was used for the following experiments.

3.2 | BSc3094 failed to reverse the decreased brain and body weight in rTg4510 mice

In agreement with previous studies,[42,43,52] we observed a pronounced decrease (≈−15%) in the total brain weight of rTg4510 mice compared to control littermate animals (Figure 2A). This correlated with a concomitant decrease (≈−9%) in the body weight (BW) of transgenic mice, monitored from the Alzet pump implantation until sacrifice. The decrease in the brain and body weight was not reversed by treatment with BSc3094 (Figure 2B).

3.3 | BSc3094 strongly reduces Tau phosphorylation in rTg4510 mice

The effect of BSc3094 in markers of Tau pathology was also assessed. rTg4510 mice treated with vehicle presented higher levels (≈80%) of phosphorylated Tau in the repeat domain at Ser262/S356 (target of protein kinase MARK and detected with 12E8 antibody), compared to control mice (Figure 3A). Treatment with BSc3094 reversed the increase in Tau phosphorylation levels in rTg4510 mice down to control level. A similar pattern was observed when analyzing the phosphorylation levels at another epitope, Ser396/Ser404 (target of several proline-directed kinases and detected by PHF-1 antibody). Due to genotype effects, already vehicle-treated transgenic mice had a pronounced increase (≈15-fold) in the phosphorylation levels at this epitope compared to control mice (Figure 3B), which was, however, reversed down to half by treatment with BSc3094 (≈7-fold).

3.4 | rTg4510 mice have no motor impairments but increased anxiety-like behavior in the open field test

Assessing motor activity in transgenic animals is important to exclude any motor impairment that may affect the result of behavioral tests that rely on locomotor activity (eg, MWM). The OF test was used to evaluate general locomotor activity levels, anxiety, and willingness to explore in the mouse models.[53] Mice display a natural aversion to bright open areas, but they have a drive to explore a perceived threatening stimulus. Increased levels of anxiety in the mice result in a decreased percentage of time in the center of the OF arena and higher preference to stay near the walls. Our results showed that rTg4510 transgenic mice did not display locomotor impairments, as no differences were found between control and transgenic mice in the distance traveled in the OF on both days of the test (Figure 4A and 4B). On the other hand, analyzing the time spent in the center of the OF arena showed that vehicle-treated rTg4510 mice spent a lower percentage

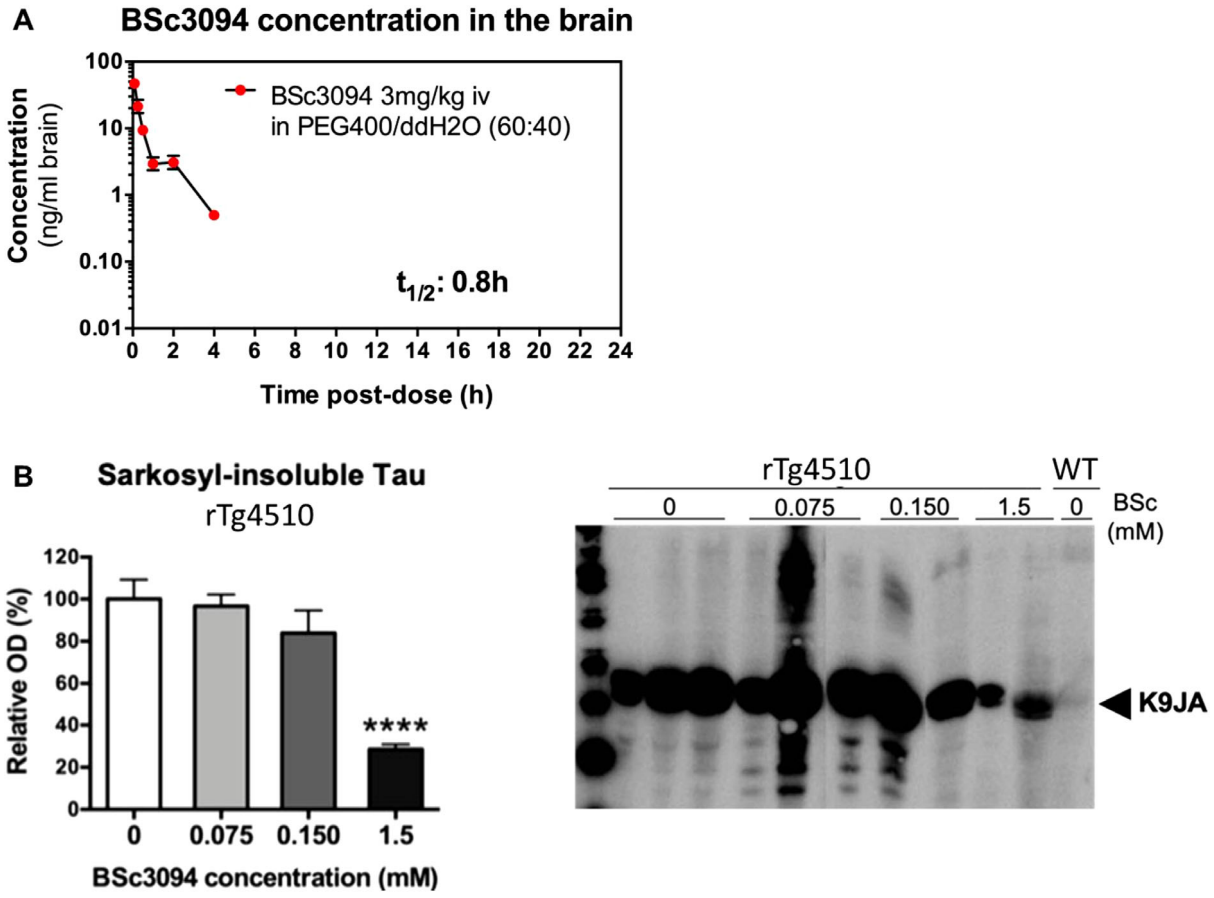

FIGURE 1 Direct intracerebral administration of BSc3094 significantly reduced sarkosyl-insoluble Tau. (A) Intravenous administration of BSc3094 (3 mg/kg in PEG400/ddH_2O (60:40)) demonstrated poor BBB permeability, as the concentration of drug in the brain was very low compared to the initial administered drug concentration, and the half-life of the drug in the brain equaled 0.8 h, meaning its potential therapeutic effect wears off in an extremely short period of time. (B) Direct intraventricular administration of three increasing doses of BSc3094 over 28 days into the brains of rTg4510 mice led to a significant reduction (≈70%) of sarkosyl-insoluble Tau achieved with the 1.5 mM drug concentration (one-way ANOVA with uncorrected Fisher's LSD post hoc test; $P < .0001$). All numerical data are shown as mean ± SEM; * denotes the significance compared to 100% (no drug). **** $P < .0001$

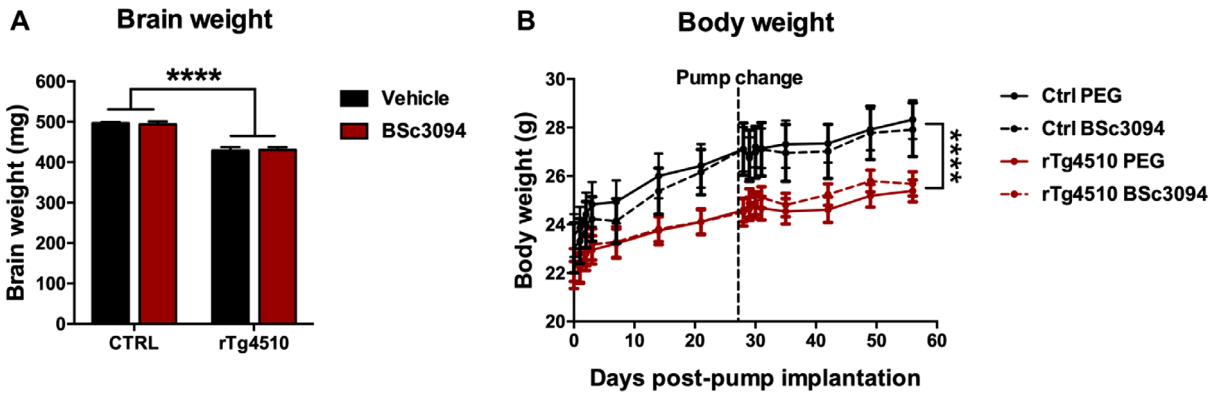

FIGURE 2 Total brain and body weight in rTg4510 and control mice used in the study. (A) Representation of the total brain weight (in mg) at the moment of sacrifice. A two-way ANOVA showed an overall effect of the genotype [$F(1, 46) = 112.8$; $P < .0001$], with double transgenic rTg4510 mice presenting a lower brain weight (≈−15%) compared to control mice. Further post hoc analysis with Tukey's multiple comparison test showed that vehicle-treated rTg4510 mice had lower brain weight than vehicle-treated controls ($P < .0001$). Similarly, BSc3094-treated rTg4510 mice also presented lower brain weight than BSc3094-treated controls ($P < .0001$). There was no effect of the drug treatment. (B) Representation of the brain weight over time, from the pump implantation until the sacrifice date, showed that double transgenic mice had a decreased brain weight compared to the control littermates [$F(1, 472) = 69.92$; $P < .0001$]. Similar to the brain weight, the drug treatment did not reverse the brain weight loss observed in the transgenic mice. All numerical data are shown as mean ± SEM; * denotes the effect of the genotype; **** $P < .0001$

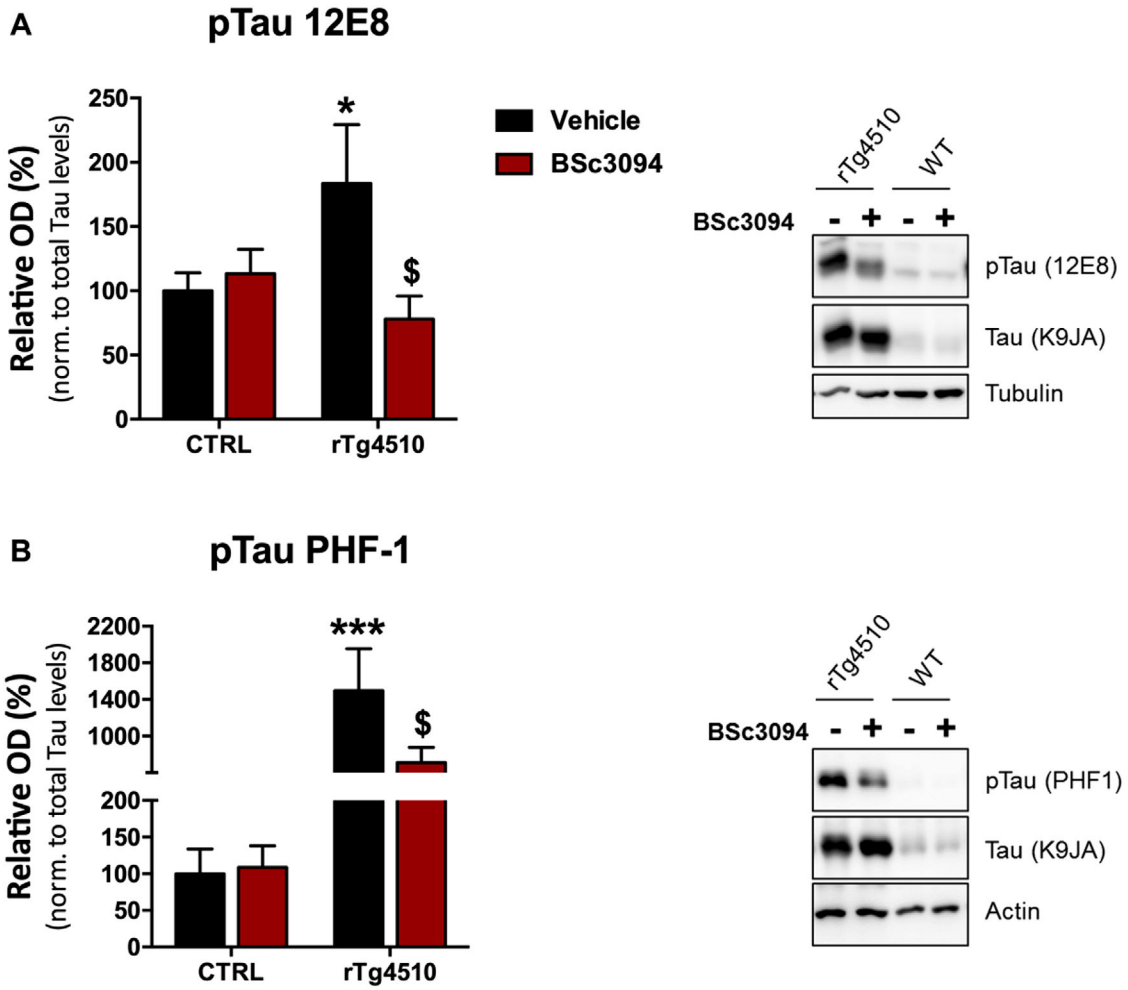

FIGURE 3 Treatment with BSc3094 reduces Tau phosphorylation in rTg4510 mice. (A) A two-way ANOVA analysis demonstrated an interaction between genotype and treatment on the levels of 12E8 [$F(1, 22) = 4.32$; $P = .0495$]. Further post hoc analysis with uncorrected Fisher's LSD test showed that rTg4510 mice presented an increase in the levels of 12E8 compared to control animals ($P = .429$), an effect that was reversed by BSc3094 treatment ($P = .0160$). (B) An overall effect of the genotype was detected regarding the levels of PHF-1 [$F(1, 22) = 14.58$; $P = .0009$]. Uncorrected Fisher's LSD post hoc test showed that the phosphorylation at the epitope Ser396/ser404, detected with PHF-1 antibody, was increased in vehicle-treated rTg4510 ≈15-fold compared to controls ($P = .0007$). This effect was reversed down to half (≈7-fold with respect to (w.r.t.) controls) by treatment with BSc3094 ($P = .0452$). All numerical data are shown as mean +/- SEM; * denotes the effect of the genotype; $ denotes the effect of BSc3094 treatment. *, $ $P < .05$; *** $P < .001$

(−40% to 50%) of time in the center of the arena compared to vehicle-treated controls on day 1 and 2 (Figure 4C, D). This phenotype was not observed in rTg4510 mice after treatment with BSc3094, showing that the drug produced a positive effect in anxiety-like behavior.

3.5 | Treatment with BSc3094 partially reverses the memory impairment in rTg4510 mice

To assess recognition memory in the experimental animals, the NOR test was performed. This test is based on the assumption that when animals are exposed to a familiar and a novel object, they typically spend more time exploring the novel rather than the familiar one, due to their natural propensity for novelty.[54] rTg4510 mice treated with vehicle spent a lower percentage of time (−20%) in the novel object during the NOR test (Figure 5A). This effect was reversed by treatment with the aggregation inhibitor, as BSc3094-treated rTg4510 mice spent a higher percentage (+20%) of time exploring the new object than vehicle-treated rTg4510 mice.

On the other hand, despite the positive results obtained in the NOR test, the drug failed to reverse the memory impairment in the y-maze test. By analyzing the arm preference in the y-maze test (Figure 5B), we observed that control mice, either treated with vehicle or BSc3094, presented a lower preference (−20%) for the old arm. Transgenic mice treated with vehicle did not show any preference for the old or new arm of the y-maze, a sign of memory impairment. This was also observed in BSc3094-treated rTg4510, showing that the drug did not reverse the memory impairments that rTg4510 mice present in the y-maze test.

Another behavioral test performed to evaluate the therapeutic effects of BSc3094 was the MWM, which assesses spatial memory

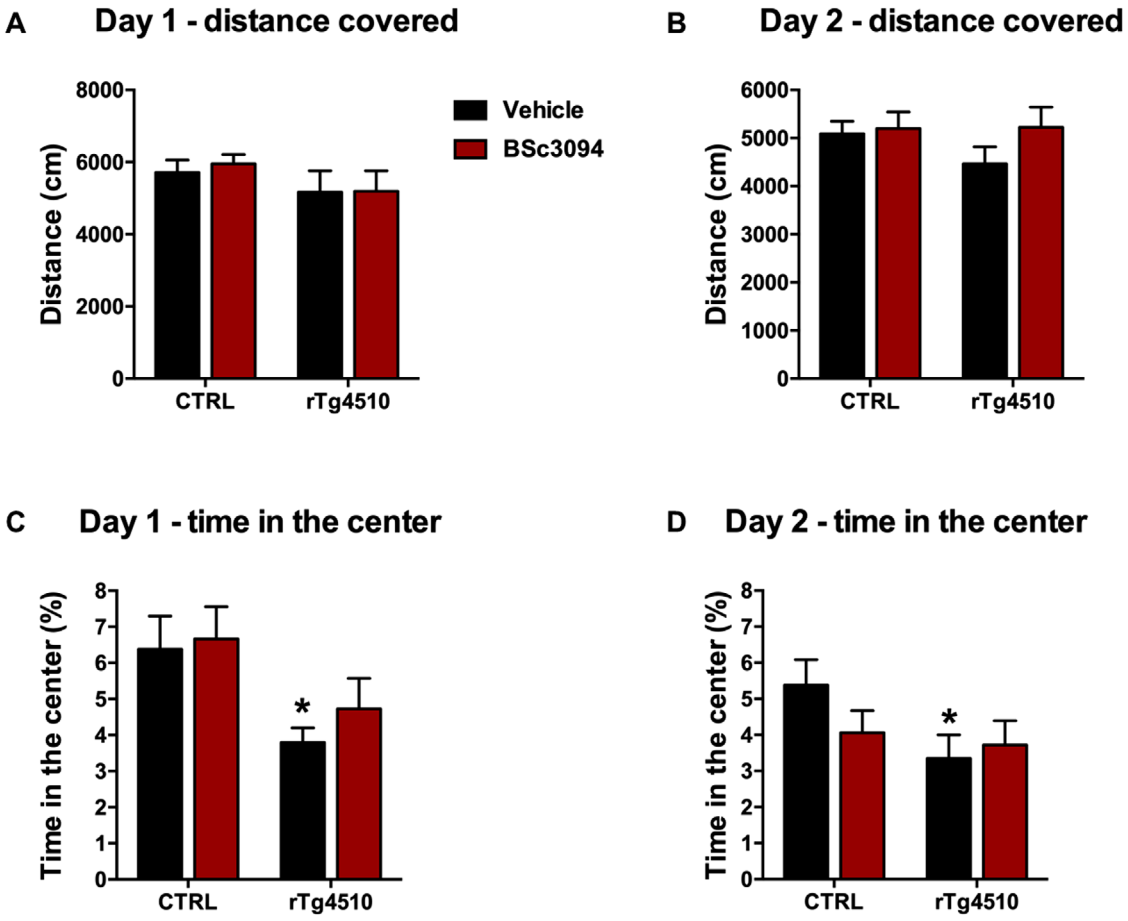

FIGURE 4 No motor impairments observed in rTg4510 mice, but an increase in anxiety-like behavior compared to control mice. rTg4510 mice presented similar distance covered values on days 1 (A) and 2 (B) of the OF test compared to control mice, showing that they did not have significant motor impairments that could affect the results of the behavioral assessment. On the other hand, an overall effect of the genotype was observed in the time spent in the center of the arena on day 1 (C) (two-way ANOVA [$F(1, 62) = 7.745$; $P = .0071$]). Uncorrected Fisher's LSD post hoc test revealed that vehicle-treated rTg4510 mice presented lower percentage of time in the center of the arena compared to vehicle-treated controls ($P = .0306$), which is an indicator of anxiety behavior. On day 2, a similar pattern was observed, with vehicle-treated rTg4510 mice presenting a lower percentage of time spent in the center of the arena (D) compared to vehicle-treated controls ($P = .0330$). This reduction in the time spent in the center of the arena was not observed in rTg4510 mice on days 1 and 2 after treatment with BSc3094, showing that the drug produced a positive effect in anxiety-like behavior. All numerical data are shown as mean ± SEM; * denotes the effect of the genotype; * $P < .05$

and learning. We observed that transgenic mice presented a higher latency to escape from the water than control mice throughout all days of learning (Figure 5C). Treatment with BSc3094 did not reverse the increased latency to escape in rTg4510 mice compared to control animals. During the probe trials (Figure 5D) the control mice, treated with either vehicle or BSc3094, spent more time in the target quadrant compared to transgenic mice, again reflecting the impaired spatial memory in rTg4510 mice. This effect was not reversed by the treatment with BSc3094 in rTg4510 mice, as no differences were observed between vehicle-treated and rTg4510-treated transgenic mice. On the other hand, analyzing the percentage of time in the target quadrant in the long-term probe trial (72 hours after the last training trial) (Figure 5E) showed that, although vehicle-treated rTg4510 mice spent a lower percentage of time in the target quadrant compared to controls, this memory impairment was partially reversed by treatment with BSc3094.

3.6 | BSc3094 has no effect on the expression of synaptic markers in rTg4510 mice

The levels of GluR1, a pre-synaptic marker playing a role in neuronal plasticity,[55] were lower (−60%) in BSc3094-treated rTg4510 mice compared to control mice (Figure 6A), showing that the anti-aggregant drug did not reverse the loss of GluR1 observed in rTg4510 mice.

In addition, we analyzed the potential effect of BSc3094 in reversing the loss of other pre- and post-synaptic markers that is usually observed in rTg4510 mice.[52] Our results showed that rTg4510 mice have lower levels of the post-synaptic marker PSD95 (Figure 6B) and pre-synaptic marker synaptophysin (Figure 6C), compared to control mice. Treatment with BSc3094 did not reverse the decrease in pre- and post-synaptic markers observed in the transgenic mice, as

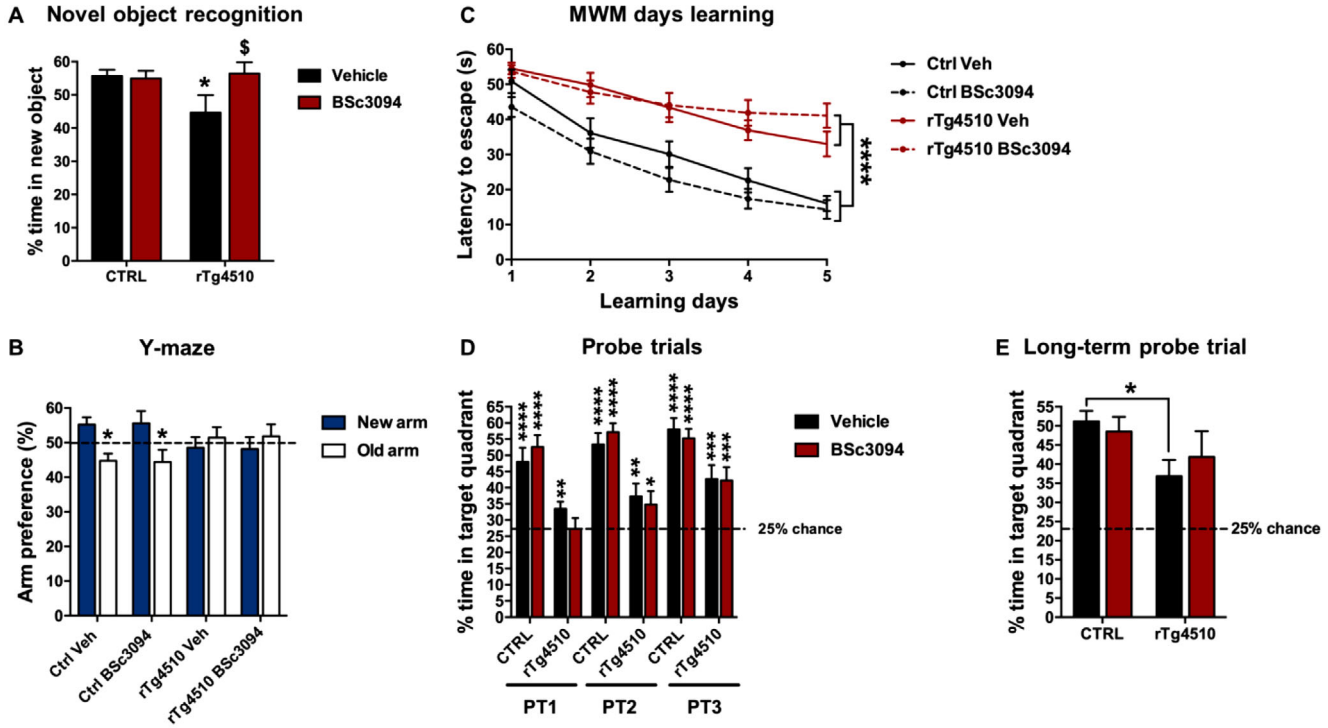

FIGURE 5 Treatment with BSc3094 partially reversed the memory deficits in rTg4510 mice. (A) Vehicle-treated rTg4510 mice spent a lower percentage (≈−20%) of time exploring the novel object in the NOR test compared to controls ($P = .0291$). The memory impairment was reversed back to control levels by the treatment with BSc3094, as drug-treated rTg4510 spent a significantly higher percentage of time exploring the novel object compared to vehicle-treated transgenic mice ($P = .0171$). Two-way ANOVA followed by uncorrected Fisher's LSD post hoc test. All numerical data are shown as mean ± SEM; * denotes the effect of the genotype; $ denotes the effect of BSc3094 treatment. *, $ $P < .05$. (B) BSc3094 did not improve spatial reference memory in rTg4510 mice. Vehicle- and BSc3094-treated control mice presented a lower preference for the old arm in the y-maze test. A two-way ANOVA revealed an interaction between genotype and treatment [$F(3,122) = 3.414$; $P = .0197$]. Post hoc analysis with uncorrected Fisher's LSD test showed a decreased preference for the old arm in vehicle-treated control mice ($P = .024$) and in BSc3094-treated control mice ($P = .0112$). In contrast, vehicle-treated rTg4510 mice showed no preference for the new or old arm reflecting impaired spatial reference memory. These deficits in the transgenic mice were not reversed by BSc3094 treatment. All numerical data are shown as mean ± SEM. * $P < .05$ when compared to new arm preference. (C) BSc3094 treatment slightly improved long-term memory in the MWM. Two-way ANOVA analysis revealed an overall effect of the genotype on the latency to escape in the MWM $F(3, 305) = 42.88$. Vehicle-treated rTg4510 mice presented a significantly increased latency to escape in the MWM test compared to vehicle-treated controls ($P < .0001$). This memory deficit was not reversed by BSc3094 treatment, as drug-treated controls ($P < .0001$). (D) By comparing the percentage of time each group spent in the target quadrant with the 25% chance of exploration we observed that transgenic mice spent a lower percentage of time in the target quadrant of the MWM in the three probe trials performed compared to control mice, an effect that was not reversed by treatment with BSc3094. (E) A two-way ANOVA analysis of the percentage of time in the target quadrant in the long-term probe trial denoted an overall effect of the genotype [$F(1, 62) = 5.309$; $P = .0246$]. Further post hoc analysis with uncorrected Fisher's LSD test showed that vehicle-treated rTg4510 mice spent a significantly lower percentage of time (−28%) in the target quadrant in the long-term probe trial compared to vehicle-treated controls ($P = .0246$), an effect that was partially reversed by BSc3094 treatment. All numerical data are shown as mean ±; * denoted the effect of the genotype in A, C, and E; in D, * denotes the significance compared to 25% chance of exploration of the target quadrant. *, $ $P < .05$; ** $P < .01$; *** $P < .001$; **** $P < .0001$

drug-treated rTg4510 mice presented lower levels of PSD95 and synaptophysin compared to control mice.

4 | DISCUSSION

The improved understanding of the physiological and pathological roles of Tau, together with advances in the development of transgenic models, has led to the identification of novel targets and drug candidates for AD. Several compounds targeting Tau have so far progressed into clinical testing, including anti-Tau vaccines and aggregation blockers (eg, methylene blue [MB]), which reverses the proteolytic stability of protease-resistant Tau filaments by blocking the Tau-Tau interaction thought the MT-binding domain.[16,17,19,56,57] However, the MB derivative LMTX did not show treatment benefit when tested at two doses in phase III trials involving 891 participants with mild-to-moderate AD,[58] for reasons that remain unclear.

Other strategies have been developed that do not target Tau directly, but targets involved in pathways with a putative role in Tau-mediated toxicity, such as MT stabilizers and small molecules to block

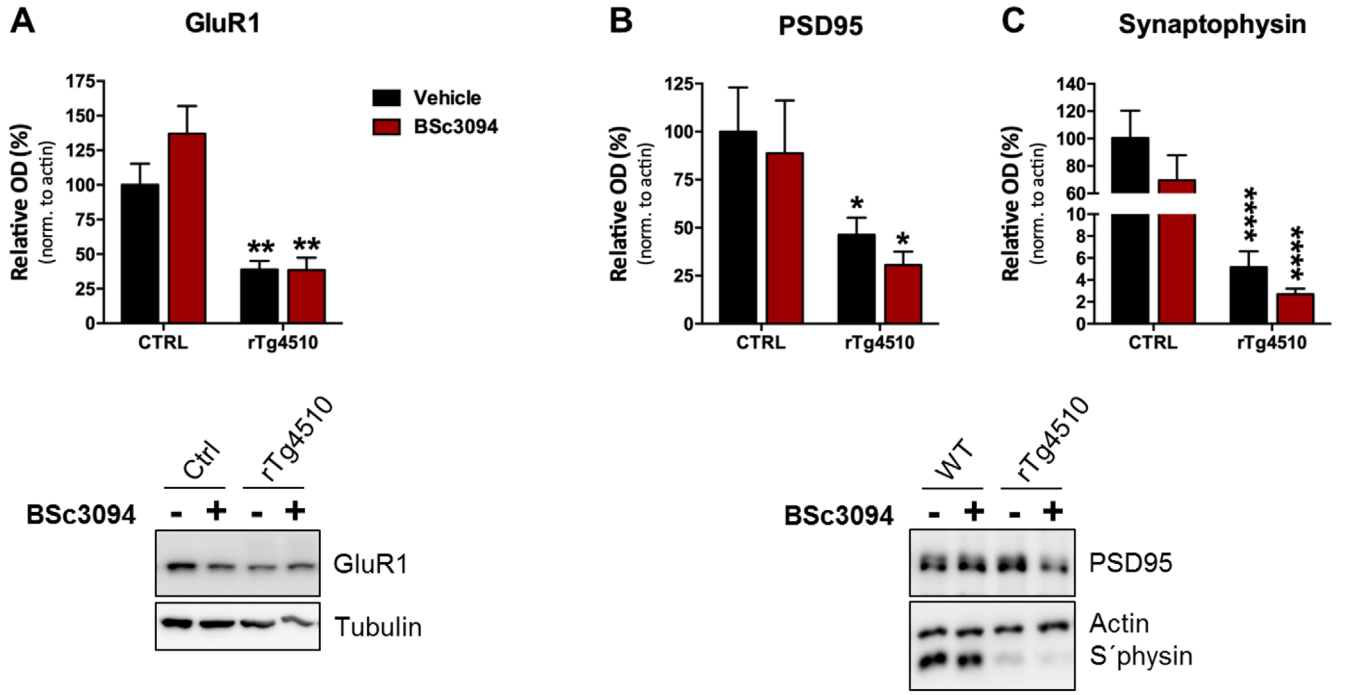

FIGURE 6 BSc3094 treatment did not reverse the loss of synaptic markers in rTg4510 mice. (A) A two-way ANOVA showed an overall effect of the genotype on the levels of GluR1 [$F(1, 22) = 35.08$; $P = .0001$]. Further uncorrected Fisher's LSD post hoc test showed that vehicle-treated rTg4510 mice presented significantly lower levels of GluR1 compared to vehicle-treated control mice ($P = .0030$), a decrease that was also observed in BSc3094-treated rTg4510 mice ($P = .0039$), demonstrating the BSc3094 fails to reverse the loss of GluR1 observed in the transgenic mice. (B) An overall effect of the genotype was observed on the levels of PSD95 [$F(1, 22) = 8.892$; $P = .0066$]. Uncorrected Fisher's LSD post hoc test revealed that vehicle-treated rTg4510 mice presented significantly lower levels of PSD95 compared to vehicle-treated control mice ($P = .0456$), a decrease that was also observed in BSc3094-treated rTg4510 mice ($P = .0153$), demonstrating that the drug treatment did not reverse the loss in the expression of PSD95. (C) Analysis of the expression of synaptophysin with two-way ANOVA showed an overall effect of the genotype [$F(1, 22) = 34{,}24$; $P < .0001$]. Further post hoc analysis with uncorrected Fisher's LSD test showed that vehicle-treated rTg4510 mice presented significantly lower levels of synaptophysin compared to control mice ($P < .0001$), an effect that was not reversed by BSc3094 treatment ($P < .0001$). All numerical data are shown as mean ± SEM; * denotes the effect of the genotype; * $P < .05$; ** $P < .01$; **** $P < .0001$

Tau hyperphosphorylation and acetylation.[59] Some examples would be MK-8719, a novel, selective, and potent O-linked N-acetylglucosamine (O-GlcNAc)-ase (OGA) inhibitor that elevates brain O-GlcNAc levels, reduces pathological Tau, and ameliorates brain atrophy in the rTg4510 mice.[60] In addition, increasing neuronal activity with an adenosine A1 receptor antagonist (rolofylline) restored Tau-induced presynaptic dysfunction as well as learning and memory impairments.[41]

Another potential inhibitor of Tau aggregation is BSc3094. Previous studies showed that this compound efficiently reduced Tau phosphorylation and aggregation (>82%), increasing at the same time cell viability and having no cytotoxic effects in N2a cells expressing pro-aggregant mutant hTau.[39,40] This cell line expresses the Tau mutation in the repeat domain, showing that BSc3094 operates at the level of this domain responsible for aggregation. Further studies showed that BSc3094 was capable of reducing the levels of insoluble Tau and increase the locomotion speed in a *C. elegans* model of tauopathy expressing pro-aggregant mutant hTau.[17] Recently, BSc3094 reversed the pre-synaptic impairment observed in organotypic hippocampal slices from pro-aggregant Tau transgenic mice, by reversing the paired-pulse depression observed in transgenic slices after applying a paired-pulse stimulus of the Schaffer collaterals.[41] Taken together, these results strengthen the hypothesis that BSc3094 or related compounds may be a potential therapeutic agent for AD, encouraging us to further test the drug in an in vivo model of strong Tau pathology, the rTg4510 mouse line.

Here, we observed that administration of BSc3094 via direct intraventricular infusion using Alzet osmotic pumps showed a reduction in the levels of sarkosyl-insoluble Tau in rTg4510 mice, compared to non-treated rTg4510 mice. Because BSc3094 is an inhibitor of Tau aggregation, it was important to select an appropriate mouse model to test this drug, with extensive NFT pathology at a young age, hence the use of rTg4510 mice. These animals overexpress human P301L Tau mutation (≈13 times the level of endogenous mouse Tau), and develop pre-tangles as early as 2.5 months of age, accompanied by impaired spatial memory.[42,43]

The brain weight of the mice, monitored weekly, was the first outcome of the treatment. BSc3094 did not reverse the brain weight loss typically observed in this transgenic mouse line. Furthermore, at the day of sacrifice, the brain weight was measured. Again, BSc3094 failed to reverse the brain weight loss characteristic in rTg4510 mice.

Previous studies showed that rTg4510 mice present a loss of 60% of CA1 neurons at 5.5 months of age, which results in a significant loss in brain weight.[42,43] A likely explanation is that pathological alterations that culminate in this extensive neuronal loss start very early in life, so that it reaches a massive reduction in CA1 cells at 5.5 months of age. Therefore, starting the treatment with BSc3094 at 2 months of age may have been too late to reverse or slow down the neuronal loss characteristic of rTg4510 mice, explaining why BSc3094-treated mice also presented a lower brain weight compared to control littermate mice.

Despite this, treatment with BSc3094 strongly reduced the levels of phosphorylated Tau (detected with both 12E8 and PHF-1 antibodies), as well as the levels of sarkosyl-insoluble Tau, which is in agreement with previous *in vitro* studies, plus an indicator that pathological hallmarks may be reduced upon BSc3094 treatment.

In addition, treatment with BSc3094 resulted in a reversal of anxiety-like behavior and improvement in certain cognitive tests. Furthermore, BSc3094 treatment reversed the memory impairment in rTg4510 mice in the NOR test, based on the assumption that mice have an innate tendency for exploring a novel environment or object. Treatment with BSc3094 also improved long-term memory in the MWM maze, as vehicle-treated rTg4510 mice spent a significantly lower percentage of time in the target quadrant during the long-term probe trial (72 hours after the last training session) compared to control mice. This was partly reversed by treatment with BSc3094, although no beneficial effect was observed on the latency to escape from the water during the MWM learning days or during the other probe trials. Besides this, BSc3094 also failed to reverse the memory deficits observed in the y-maze test, as well as the loss in synaptic markers GluR1, synaptophysin, and PSD95 in rTg4510 mice.

The failure in reversing some cognitive deficits or pathological markers may be explained by the fact that the different behavioral tasks performed to assess cognition in rTg4510 mice involve different types of memory that require distinct neuronal networks and brain regions for their storage and retrieval.[61,62] Furthermore, the extent of Tau pathology and the concentration of BSc3094 reaching each part of the mouse brain may be different, which could contribute to the differences. In addition, the implantation of Alzet osmotic pumps and brain infusion kit in young mice (2 months of age) is a delicate surgery, which may also contribute to an increased variability and the conflicting results. Moreover, the levels of mutant hTau in the rTg4510 mouse model are very high compared to the levels of endogenous mouse Tau (≈13-fold) supporting/leading to a strong Tau pathology with tangles and memory deficits at a very young age (2.5 months).[42,43] Based on this, the window for a therapeutic intervention in rTg4510 mice is short. We started the treatment as early as possible, as we wanted to avoid the development of pathological changes in the brain that may be irreversible. However, we could not start before 2 months of age because, even using the smaller model of Alzet osmotic pumps, the animals needed to weight at least 20 g to be able to cope with the subcutaneous implantation of the Alzet pump. This may have been a late start for the therapeutic intervention, which further contributes to the conflicting results.

For other treatments such as MB, it has been shown previously that depending on the level of pathology and the stage to start the treatment, a completely different outcome could arise, showing that the same drug could be more or less beneficial when applied at the right time.[19] In case continuous MB application was initiated before onset of Tau pathology, cognitive as well as synaptic functions were preserved in mice with relatively low Tau neuropathologic burden. By contrast, too late administration of MB (after onset of cognitive decline) was not able to rescue cognitive deficits or synaptic decay in these animals. In addition, MB had no effect in mice exhibiting stronger aggregation properties of Tau with faster disease progression.

In a future approach, a different mouse model that develops Tau aggregates and pathology at a later stage in life could be considered, as this would allow us to perform an earlier interventional approach. Furthermore, it would facilitate the implantation of the Alzet osmotic pump, as the use of adult animals would facilitate the experimental procedure. Another possibility would be to make use of the regulatable expression of the transgene in the rTg4510 mice. Administration of doxycycline, a tetracycline analog, would lead to the inactivation of the transgene expression, allowing the animals to grow without developing any pathological changes. This would allow us to perform the BSc3094 treatment later in life, very shortly after stopping the administration of doxycycline, ensuring that the treatment starts early enough before any pathological changes occur.

Another important aspect is the fact that, although BSc3094 treatment resulted in a strong reduction of Tau phosphorylation and in the levels of sarkosyl-insoluble Tau, there was no robust improvement in terms of synaptic markers, memory, and cognition. This suggests that Tau aggregates may not be the toxic Tau species, but intermediate forms of Tau could be causing the pathology and neurodegeneration. Indeed, although inhibiting Tau aggregation seems a valid therapeutic strategy to halt Tau-mediated neurodegeneration in AD, based on the premise that this protein has a crucial role in Tauopathies and drives pathology, this assumption has been questioned over the last years.[63–65] Currently, it is still unclear which form of Tau is pathological and if Tau aggregates are the toxic Tau species or not. If Tau aggregates are not deleterious, this means that Tau aggregation inhibitors will produce little or no effect, or even be harmful, as we may be reducing the tangle load but increasing the number of small oligomers, which are now proposed to be toxic.[63–65] However, if oligomers are, in fact, the toxic species, they occur much earlier than aggregation, and the potential beneficial effect of BSc3094 on them should be further studied.

5 | CONCLUSIONS

Our study showed that BSc3094, an inhibitor of Tau aggregation, strongly reduces Tau phosphorylation and aggregated insoluble Tau in rTg4510 mice. Furthermore, the drug also reversed the cognitive impairment typically observed in this mouse model in certain behavioral tests, despite presenting a limited effect in others (Table 1).

TABLE 1 Effect of Bsc3094 treatment on rTg4510

Target analysis	Test/Analysis	Effect of BSc3094 on rTg4510 mice
Tau	Sarkosyl-extraction	↓ Tau aggregation
	Tau phosphorylation	↓ Tau phosphorylation at Ser262/S356
		↓ Tau phosphorylation at Ser396/Ser404
Brain and body weight		= reduced brain and body weight compared to Ctrl
Behavior	Open Field	= locomotor activity
		↓ Anxiety
	NOR test	↑ object recognition memory
	MWM	↑ long-term spacial memory
	Y-maze	= decreased compared to Ctrl
Synaptic markers	GluR1	= reduced brain and body weight compared to Ctrl
	PSD95	= reduced brain and body weight compared to Ctrl
	Synaptophysin	= reduced brain and body weight compared to Ctrl

Overall, these studies add novel evidence to our understanding of the use of Tau aggregation inhibitors as potential therapeutic agents to halt the propagation of Tau pathology. In general, treatment outcomes using Tau aggregation inhibitors such as BSc3094 (or MB) appear to depend on three main parameters: (1) the aggregation propensity of (mutant) Tau, (2) the anti-aggregant potential and brain availability of the inhibitor, and (3) the time point of intervention relative to to disease progression (ie, onset of cognitive decline). It is important to note that the potential contribution of intermediate oligomeric Tau species for the development and progression of pathology cannot be excluded.[64] Given the complex pathology of AD, it can be anticipated that combinatorial and individualized treatments should be explored, which could be designed for each patient. These strategies could target Tau and Aβ, and also add agents to modulate inflammation, enhance synaptic activity, and stimulate neurogenesis and neurite regrowth. Furthermore, improving methods for drug delivery into the brain, combined with the optimization of antibody formats and specificity, would contribute to the success of therapeutic interventions.

ACKNOWLEDGMENTS

We thank the animal facilities of CAESAR research center and of the DZNE Institute, Bonn. We thank Dr. B Schmidt (Univ. Darmstadt) and Dr. M. Pickhardt (DZNE) for synthesizing BSc3094 and characterizing its effect on tau protein, and Dr. A. Schneider (DZNE) and Dr. S. Kaniyappan (DZNE) for helpful comments on the manuscript.

COMPETING INTERESTS

All authors declare that they have no competing interests concerning the present study.

ETHICS APPROVAL AND CONSENT TO PARTICIPATE

All animal experiments were carried out in accordance with the guidelines of the German Welfare Act and approved by the local authorities (Landesamt für Natur, Umwelt, und Verbraucherschutz Nordrhein-Westfalen) under the animal permission 84-02.04.2017-A405.

REFERENCES

1. Grundke-Iqbal I, Iqbal K, Tung Y-c, Quinlan M, Wisniewski HM, Bindert LI. Abnormal phosphorylation of the microtubule-associated protein tau in Alzheimer cytoskeletal pathology. *Proc Natl Acad Sci*. 1986;83(13):4913-4917.
2. Iqbal K, Liu F, Gong C-X, Grundke-Iqbal I. Tau in Alzheimer disease and related tauopathies. *Curr Alzheimer Res*. 2011;7(8):656-664.
3. Huang LK, Chao SP, Hu CJ. Clinical trials of new drugs for Alzheimer disease. *J Biomed Sci*. 2020;27(1):1-13.
4. Dehmelt L, Halpain S. The MAP2/Tau family of microtubule-associated proteins. *Genome Biol*. 2005;6(1):1-10.
5. Götz J, Xia D, Leinenga G, Chew YL, Nicholas H. What renders TAU toxic. *Front Neurol*. 2013;4(June):72-72.
6. Lopresti P, Szuchet S, Papasozomenos SC, Zinkowski RP, Binder LI. Functional implications for the microtubule-associated protein Tau: localization in oligodendrocytes. *Proc Natl Acad Sci*. 1995;92(October):10369-10373.
7. Gorath M, Stahnke T, Mronga T, Goldbaum O, Richter-Landsberg C. Developmental changes of tau protein and mRNA in cultured rat brain oligodendrocytes. *Glia*. 2001;36(1):89-101.
8. Shahani N, Brandt R. Functions and malfunctions of the Tau proteins. *Cell Mol Life Sci*. 2002;59:1668-1680.
9. Wang Y, Mandelkow E. Tau in physiology and pathology. *Nat Rev Neurosci*. 2016;17(1):5-21.
10. Braak H, Braak E. Neuropathological stageing of Alzheimer-related changes. *Acta Neuropathol (Berl)*. 1991;82(4):239-259.
11. Clavaguera F, Grueninger F, Tolnay M. Intercellular transfer of tau aggregates and spreading of tau pathology: implications for therapeutic strategies. *Neuropharmacology*. 2014;76(PART A):9-15.
12. Schneider A, Mandelkow E. Tau-based treatment strategies in neurodegenerative diseases. *Neurotherapeutics*. 2008;5(3):443-457.
13. Congdon EE, Sigurdsson EM. Tau-targeting therapies for Alzheimer disease. *Nat Rev Neurol*. 2018;14:399-415.
14. Jadhav S, Avila J, Schöll M, et al. A walk through tau therapeutic strategies. *Acta Neuropathol Commun*. 2019;7(1):22-22.
15. Lee VMY, Brunden KR, Hutton M, Trojanowski JQ. Developing therapeutic approaches to tau, selected kinases, and related neuronal protein targets. *Cold Spring Harb Perspect Med*. 2011;1:1-20.

16. Congdon EE, Wu JW, Myeku N, et al. Methylthioninium chloride (methylene blue) induces autophagy and attenuates tauopathy in vitro and in vivo. *Autophagy*. 2012;4:609-622.
17. Fatouros C, Pir GJ, Biernat J, et al. Inhibition of tau aggregation in a novel Caenorhabditis elegans model of tauopathy mitigates proteotoxicity. *Hum Mol Genet*. 2012;21(16):3587-3603.
18. Hosokawa M, Arai T, Masuda-Suzukake M, et al. Methylene blue reduced abnormal Tau accumulation in P301L Tau transgenic mice. *PLoS One*. 2012;7(12):22-23.
19. Hochgräfe K, Sydow A, Matenia D, et al. Preventive methylene blue treatment preserves cognition in mice expressing full-length pro-aggregant human Tau. *Acta Neuropathol Commun*. 2015;3(1):25-25.
20. Taniguchi S, Suzuki N, Masuda M, et al. Inhibition of heparin-induced tau filament formation by phenothiazines, polyphenols, and porphyrins. *J Biol Chem*. 2005;280(9):7614-7623.
21. Wischik CM, Harrington CR, Storey JMD. Tau-aggregation inhibitor therapy for Alzheimer's disease. *Biochem Pharmacol*. 2014;88(4):529-539.
22. DeVos SL, Miller T. Direct intraventricular delivery of drugs to the rodent central nervous system. *J Vis Exp*. 2013;50326(75):1-10.
23. Xu H, Rosler TW, Carlsson T, et al. Tau silencing by siRNA in the P301S mouse model of tauopathy. *Curr Gene Ther*. 2014;14(5):343-351.
24. Lasagna-Reeves CA, Md Haro, Hao S, et al. Reduction of Nuak1 decreases tau and reverses phenotypes in a tauopathy mouse model. *Neuron*. 2016;92(2):407-418.
25. Boutajangout A, Ingadottir J, Davies P, Sigurdsson EM. Passive immunization targeting pathological phospho-tau protein in a mouse model reduces functional decline and clears tau aggregates from the brain. *J Neurochem*. 2011;118(4):658-667.
26. Chai X, Wu S, Murray TK, et al. Passive immunization with anti-tau antibodies in two transgenic models: reduction of tau pathology and delay of disease progression. *J Biol Chem*. 2011;286(39):34457-34467.
27. Kontsekova E, Zilka N, Kovacech B, Novak P, Novak M. First-in-man tau vaccine targeting structural determinants essential for pathological tau-tau interaction reduces tau oligomerisation and neurofibrillary degeneration in an Alzheimer's disease model. *Alzheimer's Res Ther*. 2014;6(4):1-12.
28. Novak P, Schmidt R, Kontsekova E, et al. Safety and immunogenicity of the tau vaccine AADvac1 in patients with Alzheimer's disease: a randomised, double-blind, placebo-controlled, phase 1 trial. *Lancet Neurol*. 2017;16(2):123-134.
29. Gong C-X, Grundke-Iqbal I, Iqbal K. Targeting Tau protein in Alzheimer's disease. *Drugs Aging*. 2010;27:351-365.
30. Le Corre S, Klafki HW, Plesnila N, et al. An inhibitor of tau hyperphosphorylation prevents severe motor impairments in tau transgenic mice. *Proc Natl Acad Sci*. 2006;103(25):9673-9678.
31. Ding H, Dolan PJ, Johnson GVW. Histone deacetylase 6 interacts with the microtubule-associated protein tau. *J Neurochem*. 2008;106(5):2119-2130.
32. Kilgore M, Ca Miller, Fass DM, et al. Inhibitors of class 1 histone deacetylases reverse contextual memory deficits in a mouse model of Alzheimer's disease. *Neuropsychopharmacology*. 2010;35(4):870-880.
33. Tran HT, Sanchez L, Brody DL. Inhibition of JNK by a peptide inhibitor reduces traumatic brain injury-induced tauopathy in transgenic mice. *J Neuropathol Exp Neurol*. 2012;71(2):116-129.
34. Ozcelik S, Fraser G, Castets P, et al. Rapamycin attenuates the progression of tau pathology in P301S Tau transgenic mice. *PLoS One*. 2013;8(5):2-8.
35. Frederick C, Ando K, Leroy K, et al. Rapamycin ester analog CCI-779/Temsirolimus alleviates tau pathology and improves motor deficit in mutant tau transgenic mice. *J Alzheimers Dis*. 2015;44(4):1145-1156.
36. Zhang B, Maiti A, Shively S, et al. Microtubule-binding drugs offset tau sequestration by stabilizing microtubules and reversing fast axonal transport deficits in a tauopathy model. *Proc Natl Acad Sci*. 2005;102(1):227-231.
37. Miyasaka T, Xie C, Yoshimura S, et al. Curcumin improves tau-induced neuronal dysfunction of nematodes. *Neurobiol Aging*. 2016;39:69-81.
38. Pickhardt M, Larbig G, Khlistunova I, et al. Phenylthiazolyl-hydrazide and its derivatives are potent inhibitors of τ aggregation and toxicity in vitro and in cells. *Biochemistry*. 2007;46(35):10016-10023.
39. Pickhardt M, Biernat J, Hübschmann S, et al. Time course of Tau toxicity and pharmacologic prevention in a cell model of Tauopathy. *Neurobiol Aging*. 2017;57:47-63.
40. Pickhardt M, Neumann T, Schwizer D, et al. Identification of small molecule inhibitors of Tau aggregation by targeting monomeric Tau as a potential therapeutic approach for tauopathies. *Curr Alzheimer Res*. 2015;12(9):814-828.
41. Dennissen F, Anglada-Huguet M, Sydow A, Mandelkow E, Mandelkow E-M. Adenosine A 1 receptor antagonist rolofylline alleviates axonopathy caused by human Tau ΔK280. *Proc Natl Acad Sci*. 2016;113(41):11597-11602.
42. Ramsden M, Kotilinek L, Forster C, et al. Age-dependent neurofibrillary tangle formation, neuron loss, and memory impairment in a mouse model of human tauopathy (P301L). *J Neurosci*. 2005;25(46):10637-10647.
43. SantaCruz K, Lewis J, Spires T, et al. Tau suppression in a neurodegenerative mouse model improves memory function. *Science*. 2005;309(5733):476-481.
44. Deacon RMJ. Assessing nest building in mice. *Nat Protoc*. 2006;1(3):1117-1119.
45. Deacon RMJ. Assessing burrowing, nest construction, and hoarding in mice. *J Vis Exp*. 2012;59:e2607-e2607.
46. Deacon RMJ. Burrowing: a sensitive behavioral assay, tested in five species of laboratory rodents. *Behav Brain Res*. 2009;200(1):128-133.
47. Sydow A, Hochgräfe K, Könen S, et al. Age-dependent neuroinflammation and cognitive decline in a novel Ala152Thr-Tau transgenic mouse model of PSP and AD. *Acta Neuropathol Commun*. 2016;4:17-17.
48. Sydow A, Van der Jeugd A, Zheng F, et al. Tau-induced defects in synaptic plasticity, learning, and memory are reversible in transgenic mice after switching off the toxic Tau mutant. *J Neurosci*. 2011;31(7):2511-2525.
49. D'Hooge R, Lüllmann-Rauch R, Beckers T, et al. Neurocognitive and psychotiform behavioral alterations and enhanced hippocampal long-term potentiation in transgenic mice displaying neuropathological features of human alpha-mannosidosis. *J Neurosci*. 2005;25(28):6539-6549.
50. Greenberg SG, Davies P. A preparation of Alzheimer paired helical filaments that displays distinct tau proteins by polyacrylamide gel electrophoresis. *Proc Natl Acad Sci*. 2006;87(15):5827-5831.
51. Mocanu MM, Nissen A, Eckermann K, et al. The potential for beta-structure in the repeat domain of tau protein determines aggregation, synaptic decay, neuronal loss, and coassembly with endogenous tau in inducible mouse models of tauopathy. *J Neurosci*. 2008;28(3):737-748.
52. Helboe L, Egebjerg J, Barkholt P, Volbracht C. Early depletion of CA1 neurons and late neurodegeneration in a mouse tauopathy model. *Brain Res*. 2017;1665:22-35.
53. Seibenhener ML, Wooten MC. Use of the open field maze to measure locomotor and anxiety-like behavior in mice. *J Vis Exp*. 2015;3(96):1-6.
54. a Ennaceur. One-trial object recognition in rats and mice: methodological and theoretical issues. *Behav Brain Res*. 2010;215(2):244-254.
55. Kopec CD, Real E, Kessels HW, Malinow R. GluR1 links structural and functional plasticity at excitatory synapses. *J Neurosci*. 2007;27(50):13706-13718.
56. Wischik CM, Edwards PC, Lai RYK, Roth M, Harrington CR. Selective inhibition of Alzheimer disease-like tau aggregation by phenothiazines. *Proc Natl Acad Sci*. 1996;93(20):11213-11218.

57. van Bebber F, Paquet D, Hruscha A, Schmid B, Haass C. Methylene blue fails to inhibit Tau and polyglutamine protein dependent toxicity in zebrafish. *Neurobiol Dis*. 2010;39(3):265-271.
58. Gauthier S, Feldman HH, Schneider LS, et al. Efficacy and safety of tau-aggregation inhibitor therapy in patients with mild or moderate Alzheimer's disease: a randomised, controlled, double-blind, parallel-arm, phase 3 trial. *Lancet*. 2016;388(10062):2873-2884.
59. Li C, Götz J. Tau-based therapies in neurodegeneration: opportunities and challenges. *Nat Rev Drug Discovery*. 2017;16(12):863-883.
60. Wang X, Li W, Marcus J, et al. MK-8719, a novel and selective O-GlcNAcase inhibitor that reduces the formation of pathological tau and ameliorates neurodegeneration in a mouse model of tauopathy. *J Pharmacol Exp Ther*. 2020;374(2):252-263.
61. Thompson RF, Kim JJ. Memory systems in the brain and localization of a memory. *Proc Natl Acad Sci*. 1996;93(24):13438-13444.
62. Ben-Yakov A, Dudai Y, Mayford MR. Memory retrieval in mice and men. *Cold Spring Harb Perspect Biol*. 2015;7(12):1-28.
63. Cheng IH, Scearce-Levie K, Legleiter J, et al. Accelerating amyloid-beta fibrillization reduces oligomer levels and functional deficits in Alzheimer disease mouse models. *J Biol Chem*. 2007;282(33):23818-23828.
64. Kaniyappan S, Chandupatla RR, Mandelkow E-M, Mandelkow E. Extracellular low-n oligomers of tau cause selective synaptotoxicity without affecting cell viability. *Alzheimer's Dement*. 2017;13(11):1270-1291.
65. Necula M, Kayed R, Milton S, Glabe CG. Small molecule inhibitors of aggregation indicate that amyloid beta oligomerization and fibrillization pathways are independent and distinct. *J Biol Chem*. 2007;282(14):10311-10324.

How to cite this article: Anglada-Huguet M, Rodrigues S,Hochgräfe K, Mandelkow E, Mandelkow E-M Inhibition of Tau aggregation with BSc3094 reduces Tau and decreases cognitive deficits in rTg4510 mice. *Alzheimer's Dement*. 2021;7:e12170.https://doi.org/10.1002/trc2.12170